Proceedings of the FLC Zurich 2006
15th – 16th March 2006, IVP, ETH Zurich, Switzerland

EFFECTIVE EVALUATION OF FLC-TESTS WITH THE OPTICAL IN-PROCESS STRAIN ANALYSIS SYSTEM *AUTOGRID®*

Feldmann, Peter; Schatz, Marko

ViALUX Messtechnik + Bildverarbeitung GmbH, Reichenhainer Str. 88, D-09126 Chemnitz
TU Dresden, Institut für Produktionstechnik, George-Bähr-Str. 3c, D-01069 Dresden

ABSTRACT

The basics of FLC tests using in-process recording are described and some typical realized examples with *AutoGrid®* vario systems are illustrated. It is given an introduction how to use the *AutoGrid®* system for the effective evaluation of FLC tests. An algorithm for the automatic determination of the beginning of material failure (local necking followed by the crack) is described.

Keywords: FLC, sheet metal, formability, optical 3D strain analysis, in-process recording

1. INTRODUCTION

The development of image recording and processing techniques in the last 10 years opens a lot of new possibilities in optical strain analysis compared to the old way: manual measurement of circle grids after deformation. One of these new possibilities is the photogrammetrical 3D-measurement with a precalibrated camera setup during forming processes under the assumption, that the forming surface with it's markings is visible for the cameras. Normally in material formability tests like the tensile, the bulge or the FLC test this assumption is fulfilled. But without in-process recording the test operators try to stop the forming process of the FLC test immediately after beginning of the material failure (necking/cracking) so that the first small crack is visible. In this state strains are measured around the crack.

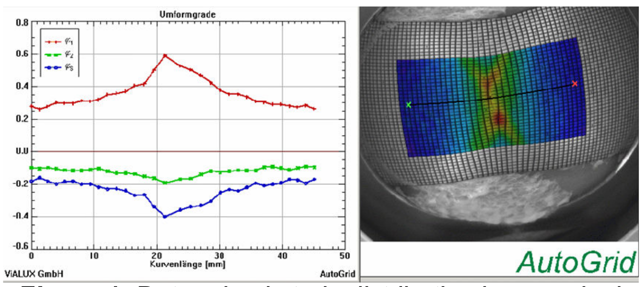

Figure 1: Determined strain distribution in a cracked specimen

Beside the difficulty to calculate accurate strains in the direct neighborhood of the crack: It is very complicated to define a value for the FLC from these results. Of course near the crack the determined strains are too high because of local necking. One way to determine FLC-value-pairs with the help of an evaluation algorithm uses crossing intersections is described in the ISO-Draft 12004 of the German and French IDDRG FLC working groups. But all involved specialists know about the difficulties on this way. The best way would be to determine the FLC-value-pairs in that moment just before the material failure starts. But for this aim in-process recording with capability of strain analysis is needed.

2. FLC TESTS WITH IN-PROCESS RECORDING

The basic idea is shown in fig. 2: A precalibrated setup of cameras (for higher measuring accuracy and stability and for better covering of curved 3D-surfaces *AutoGrid®* uses 4 cameras) records synchronized image sequences e.g. with a frame rate of 10 image sets per second. If some other measuring signals exist in the given testing environment, they can be recorded simultaneously.

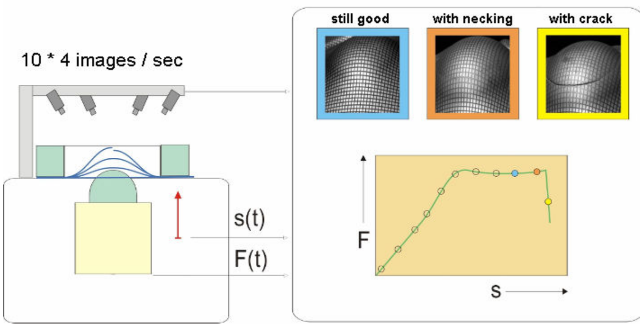

Figure 2: Principle of in-process recording of image sequences and measuring signals on testing machine

In the next 2 figures the in-process recording *AutoGrid*® *vario* system is mounted on different sheet metal testing machines.

Figure 3: The *AutoGrid*® *vario* system and the sheet metal testing machine of Erichsen comp. as an integrated solution on the EuroBLECH 2004 show

Figure 4: The *AutoGrid*® *vario* system working with an sheet metal testing machine of Roell/Amsler

The same principle works of course also in any other testing environment, e.g. for tensile or bulge tests. Fig. 5 shows the use of an in-process recording *AutoGrid*® *vario* system mounted in a special designed (distance elements) FLC-testing tool in a normal press machine.

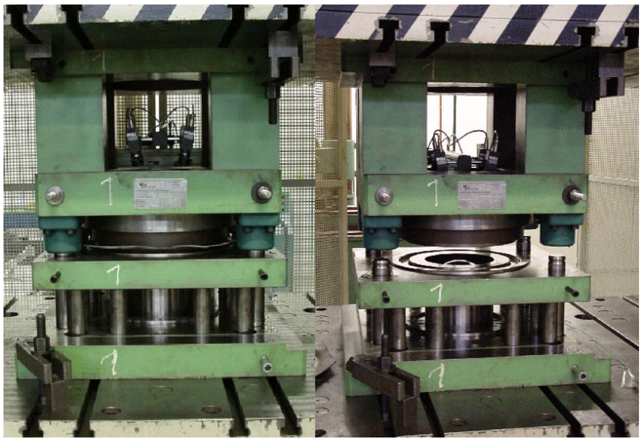

Figure 5: The *AutoGrid*® *vario* system in a special designed testing tool in a normal press machine

Figure 6 shows a screenshot of the *AutoGrid*® software after simultaneously recording of image sequences and measuring signals like punch force and displacement. The displayed moment of the image sequence is the last picture set of this sequence, when the crack becomes visible. The image sequence over the approx. last 5 seconds before the crack appears gives the possibility to determine that picture set, just before the failure of the material – the local necking followed by the crack – starts.

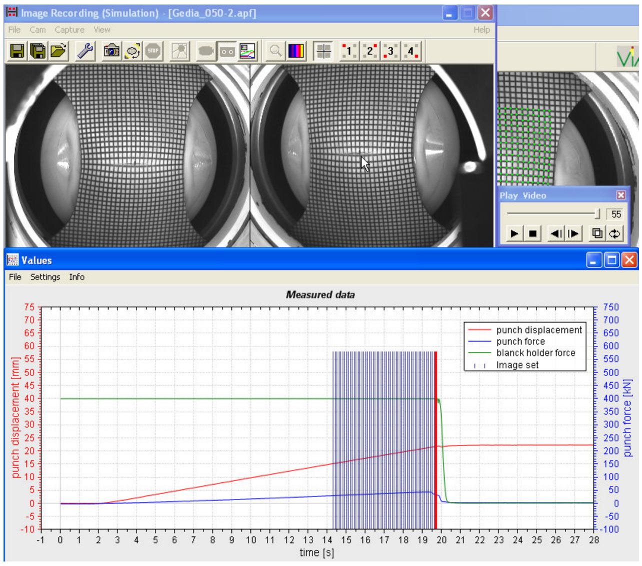

Figure 6: Screenshot with displayed pictures of cam 1 and 2 and time course of the measured signals

The identification of the last image set before the material failure starts now becomes the central question of this presentation. It is possible to analyze the whole recorded image sequence in a few minutes. In fig. 7 the results of a moment before the local necking starts are shown. In black color the strain paths of 2 neighbored points are shown. It is visible, that the point with the highest major strain value φ_1 till the end of the analyzed image sequence becomes higher and higher and the steps becomes larger and larger. But it is not possible to identify one step, when the step width becomes larger dramatically. So this way will not solve the "local-necking-start-identification-problem".

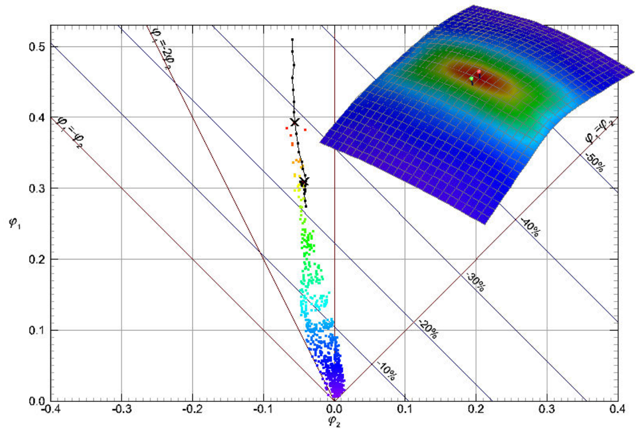

Figure 7: Strain results before start of the local necking including the strain paths of 2 marked points

But let's have a look at the strain path of the second marked point directly neighbored to the "maximum point". This strain path reaches his maximum not at the end of the analyzed sequence. In the last steps it is approx. constant. And this seems a very clear signal: At the beginning of the analyzed image sequence the major strain value gets larger and larger and then it stops. This makes sense: When the local necking starts the elongation towards the necking area in the direct neighborhood has to stop. In fig. 8 incremental strains during local necking are shown. This makes it clear: A necking zone (green marking) consists of the thin local necking area itself (red) and accompanied stopping areas (light blue) on both sides of the necking area. This all is shown very clearly in the results of in-process recorded image sequences.

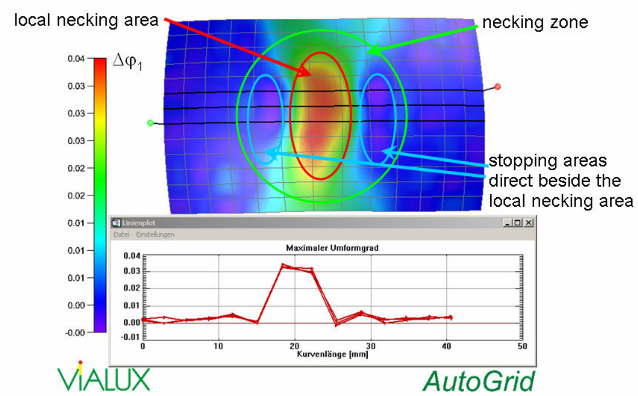

Figure 8: Incremental major strain during the necking: stopping areas on both sides of the necking area

So there are two signals we can use to identify the local necking start image set: The increasing major strain in the center of the necking area and the stopping major strain in the direct neighbored areas. So it is very easy for the experienced user to identify the start of local necking. And he can check his selection directly in the images of the recorded sequence. So this is really reliable.

3. ALGORITHM TO IDENTIFY THE START OF LOCAL NECKING AUTOMATICALLY

In this chapter an algorithm for automatic identification of the last image set before the local necking is started is described. This algorithm should fulfill the following demands:

- independent of any operator;
- work fully automatically and stabile;
- high reliability based on internal reliability checks;
- applicable on a wide range of typical materials and
- easy to understand and to use.

Actually this algorithm exists as a macros using Excel sheet. So the algorithm can be tested by interested users with their own data basis.

Step 1

Selection of the last image set before the crack (time sequence). This set normally shows a clear local necking but still no signs of a crack. The crack position has to be marked over maximum 5 coherent grid stitches.

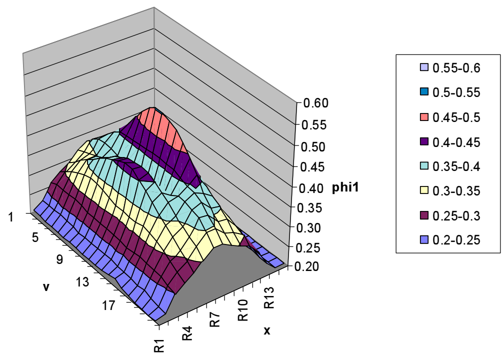

Figure 9: Marking of the crack in the last step before the crack.

Step 2

Evaluation of image sequence of at least 20 image sets before the crack (time sequence).

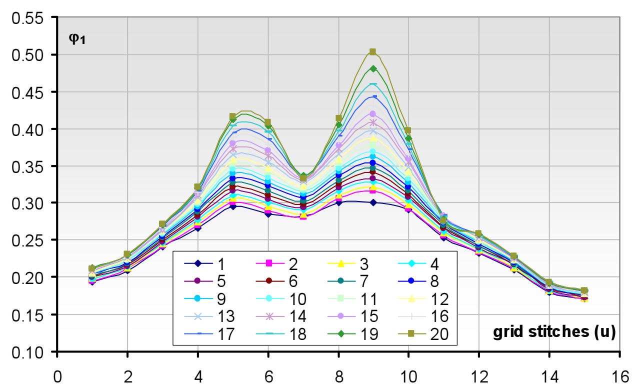

Figure 10: Major strain along intersection lines perpendicular to the crack.

Step 3

Determination of 3 coherent points with the highest middle value (over these 3 coherent points) of major strain in the direct marked crack area. Calculation of major strain middle values for all point triples on both sides of the determined maximum point triple. Figure 10 shows these middle values (for easier understanding): The growth of major strain phi 1 is tracked in the field of the later crack ("maximum") and the fields on both sides from that ("stopping environment") over time. With the beginning of the local necking in the maximum, the increase in major strain phi 1 in the environment stays behind. The determination of the fields with stopping deformation occurs to both sides of the maximum. In the chosen example in Figure 10 is it at “u=7” on the left and “u=11” on the right side.

In fig. 11 the time courses of the middle values of major strain and their time increments are shown. So it gets clear that starting from the maximum in the center “u=7” on the left and “u=11” on the right side are the first lines, where the deformation stops. We have to use them for the next steps.

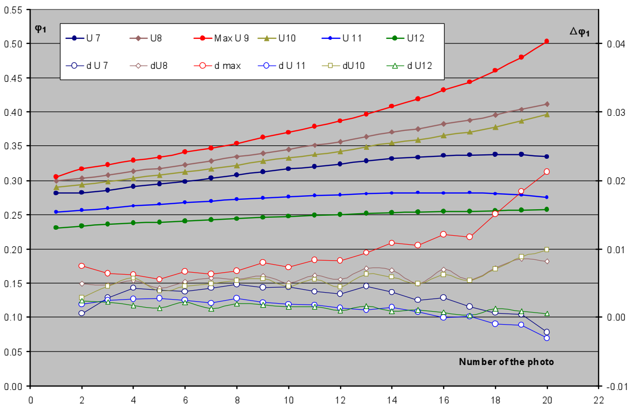

Figure 11: Time courses of mean values and increments

Step 4

To use both signals (running maximum and stopping areas) now the differences of the deformations between the maximum and the environment left and right are calculated.

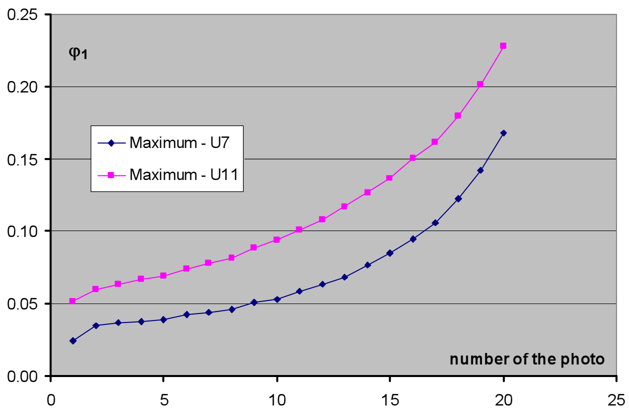

Figure 12: Time course of the differences of the major strains (maximum - left side; maximum - right side)

Step 5

<u>Assumption:</u> The rise of these differences is linear in the period before the beginning of local necking. It increases progressively with the beginning of local necking.

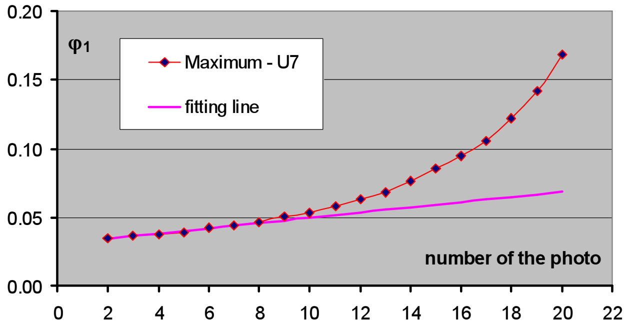

Figure 13: Fitting line by the first 7 values.

With the step-by-step calculation of the correlation coefficient, the field in the process of the differences in which a linear rise of the major strain phi 1 occurs is determined. Fig. 13 shows the fitting line for 7 values. The processes of correlation coefficients of both sides are represented in Fig. 14. The peak values are marked. The linear field is determined up to the maximum of the correlation coefficient. So the number of points for the calculation of the fitting line for the linear increasing period is determined for both sides. In the case, that the correlation coefficient is lower than “0.9”, the automatic algorithm stops because of low reliability: It seems, that in such a concrete case the above assumption is not valid.

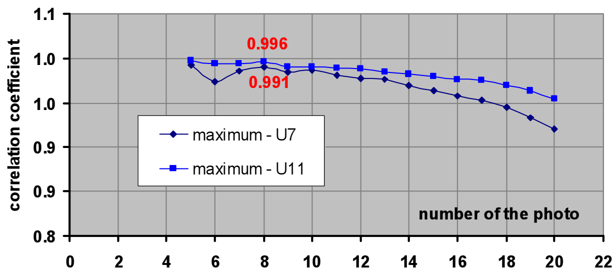

Figure 14: Correlation coefficient of both sides above the number of the considered values.

Step 6

Now we need a value for the typical material, experimental and measuring scatter of these differences. For this purpose we calculate the standard deviation of the increments of major strain in the determined linear field.

Step 7

For the fixing of the image set before the material failure starts, an upper boundary is defined parallel to the linear fitting line shifted three times of standard deviation upwards. The first image set over this upper boundary is fixed as the image set with starting local necking. So one image set before is the image set for the respective side. In fig. 15 image set 11 is the first over the upper boundary and for this left side we had to choose the 10th image set.

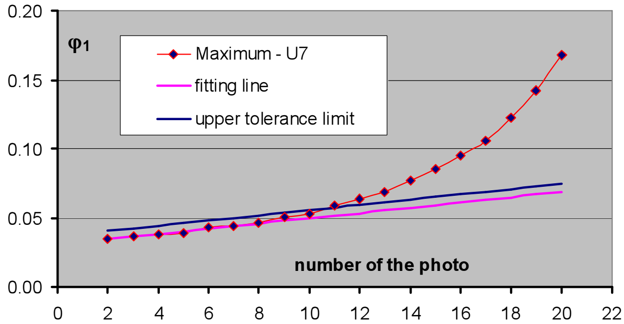

Figure 15: upper tolerance line parallel to the fitting line for the linear field

In the same way it has to be done for the other side (in our given example: maximum – u11). So in this algorithm is an independent reliability check included: If we get the same image set for both sides, the reliability is very high. If we get different image sets, the determination of the FLC-values takes place on that side, where the linear field could be described with the higher correlation coefficient. Furthermore the information about different numbers of selected image sets on both sides can be observed by the operator.

Calculation of FLC-value-pairs

On this way the image set before the material failure starts is determined. In the marked area of the crack (step 1) the middle value of the maximum of 3 (2.0-mm grid) or 2*6 (1.0-mm grid) coherent points gives the major strain value for the FLC. From these points also has to calculated the middle value of the minor strain as the minor strain of the FLC-value-pair.